J. Phys. Chem. **1988,** *92,* 141-147

Computational Studies of the Bimolecular Reaction Dynamics of the $C_2H_4 + F_2$ System

Lionel M. Raff

Department of Chemistry, Oklahoma State University, Stillwater, Oklahoma 74078

(Received: May 5, 1987; In Final Form: July 20, 1987)

The bimolecular reaction dynamics of $C_2H_4 + F_2$ on a previously described potential energy surface have been investigated by using quasi-classical trajectory methods. All important reaction channels are open on this potential surface, and the calculated equilibrium geometries, reaction exothermicities, and fundamental vibration frequencies are in fair-to-good accord with measured values. The major reaction products are found to be either $CH_2CH_2F + F$ or $CH_2{=}CHF + HF$. 1,2-Difluoroethane is found as a reaction intermediate leading to $CH_2{=}CHF + HF$ but is never observed as a final product. The calculated reaction cross sections are all less than 5 Å^2 even for translational energies more than 1 eV in excess of the reaction threshold. Almost all of the reaction exothermicity is partitioned into the internal modes of CH_2CH_2F or $CH_2{=}CHF$. Very little of this energy appears as relative translational motion of the products. HF is usually formed in the $v = 0$, 1, or 2 vibrational state. The calculated center-of-mass differential cross section for fluorine atom scattering shows a strong backward component along with an isotropic component. The first of these is shown to arise from a direct reaction mechanism; the second is the result of complex formation. Formation of fluoroethylene is shown to occur via a complex mechanism involving formation of 1,2-difluoroethane as an intermediate. The calculated thermal rate coefficients for CH_2CH_2F and $CH_2{=}CHF$ formation are $1.38 \times 10^{14} \exp[-13\,600/RT]$ and $1.90 \times 10^{13} \exp[-11\,040/RT]$ cm^3/(mol·s), respectively. There is some suggestion of mode-specific rate enhancement for the reaction leading to CH_2CH_2F but not for the formation of $CH_2{=}CHF$. In the first case, the C–H stretching modes are found to be the most effective in enhancing the rate. The results are compared and contrasted with gas-phase data reported by Kapralova et al. and with the matrix isolation results obtained by Frei et al.

I. Introduction

Frei, Fredin, and Pimentel[1] have reported the results of studies of various photochemically assisted bimolecular reactions in cryogenic matrices. It was found that the reaction products obtained under matrix isolation conditions were often different from those obtained in the gas phase or in solution. Several of the systems investigated exhibited mode-specific rate enhancement. One such system is the addition of molecular fluorine to ethylene. Upon vibrational excitation in a cryogenic matrix, this reaction was observed to form 1,2-difluoroethane, which subsequently was stabilized by energy transfer to the matrix or decomposed to yield hydrogen fluoride and fluoroethylene:

$$C_2H_4 + F_2 \rightarrow [CH_2FCH_2F]^* \qquad (R1)$$

$$[CH_2FCH_2F]^* + M \rightarrow CH_2FCH_2F + M \qquad (R2)$$

$$[CH_2FCH_2F]^* \rightarrow CH_2{=}CHF + HF \qquad (R3)$$

M represents the matrix

The relative rates of reactions R2 and R3 are dependent upon the nature of the matrix material. The quantum efficiency for formation of 1,2-difluoroethane is found to increase 5 orders of magnitude as the photon wavenumber increases from 953 to 4209 cm^{-1}. However, the increase is neither smooth nor monotonic. There appears to be mode-specific rate enhancement in that excitation of the $v_2 + v_{12}$ combination band of C_2H_4 at 3076 cm^{-1} results in a quantum efficiency greater than that for excitation of v_9 at 3105 cm^{-1}. Knudsen and Pimentel[2] have reported similar results for the reaction of allene with F_2 in N_2, Ar, Kr, and Xe matrices at 12 K.

In contrast to the matrix isolation results, the gas-phase reaction of fluorine with olefins has been shown to involve an initiation step to form a fluoro radical.[3-5] Kapralova, Chaikin, and Shilov[3] have used a diffusion flame method to examine the addition of F_2 to ethylene between 300 and 437 K. They propose that the initial reaction steps are

$$F_2 + C_2H_4 \rightarrow CH_2CH_2F + F \qquad (R4)$$

$$F + C_2H_4 \rightarrow CH_2CH_2F \qquad (R5)$$

An activation energy and frequency factor for reaction R4 were reported.

The above results make it clear that the gas-phase reaction dynamics must be very different from those observed under matrix isolation conditions. We have previously shown that the reaction dynamics of vibrationally excited van der Waals complexes are intermediate between those observed for gas-phase bimolecular reactions and the corresponding system when matrix isolated. The van der Waals complex resembles the matrix system in that the molecules are held in close proximity with the individual molecular rotations partially quenched. It resembles the bimolecular system in that there are no third bodies to which vibrational energy may be transferred, and the van der Waals binding forces are much less efficient in holding the molecules together than is a cryogenic matrix. As a result, we have found that the $O_3 \cdot NO$ complex exhibits mode-specific rate enhancement for reaction to form $O_2 + NO_2$ products, for vibrational predissociation (VP), and for intermode energy transfer.[6] Structure specificity is also observed. We are currently studying the dynamics of the $O_3 \cdot NO$ system under matrix isolation conditions. However, comparison of the results with experiment will be difficult since the presence of a "dark reaction" of the $O_3 \cdot NO$ complex complicates the interpretation of the matrix isolation results.[7] This problem does not exist for the ethylene–fluorine system.

We have recently reported the formulation of a semiempirical potential energy surface for the $C_2H_4F_2$ system.[8] Most of the major reaction channels are open on this surface. In addition, the accuracy of the surface is such that equilibrium structures, reaction endo- and exothermicities, fundamental vibration frequencies, and some measured activation energies are predicted with fair-to-excellent accuracy. Using this surface, we may in-

---

(1) (a) Frei, H.; Fredin, L.; Pimentel, G. C. *J. Chem. Phys.* **1981**, *74*, 397. (b) Frei, H.; Pimentel, G. C. *J. Chem. Phys.* **1983**, *78*, 3698.

(2) Knudsen, A. K.; Pimentel, G. C. *J. Chem. Phys.* **1983**, *78*, 6780.

(3) Kapralova, G. A.; Chaikin, A. M.; Shilov, A. E. *Kinet. Katal.* **1967**, *8*, No. 3.

(4) (a) Miller, W. T.; Dittman, A. L. *J. Am. Chem. Soc.* **1956**, *78*, 2793. (b) Miller, W. T.; Koch, S. D. *J. Am. Chem. Soc.* **1957**, *79*, 3084. (c) Rodgers, A. S. *J. Phys. Chem.* **1963**, *67*, 2799; **1965**, *69*, 254.

(5) (a) Kapralova, G. A.; Shilov, A. E. *Kinet. Katal.* **1961**, *2*, 362. (b) Kapralova, G. A.; Rusin, A. Yu.; Chaikin, A. M.; Shilov, A. E. *Dokl. Akad. Nauk SSSR* **1963**, *150*, 1282.

(6) Arnold, C.; Gettys, N. S.; Thompson, D. L.; Raff, L. M. *J. Chem. Phys.* **1986**, *84*, 3803.

(7) Lucas, D.; Pimentel, G. C. *J. Phys. Chem.* **1979**, *83*, 2311.

(8) Raff, L. M. *J. Phys. Chem.* **1987**, *91*, 3266.

0022-3654/88/2092-0141$01.50/0

vestigate and compare the reaction dynamics for gas-phase bimolecular collisions, for VP of the excited $C_2H_4F_2$ van der Waals complex, and for the system isolated in a cryogenic matrix. In this paper, we report the results of classical trajectory studies of the first of these. Later papers will deal with intramolecular energy-transfer processes, unimolecular dissociation reactions of 1,2-difluoroethane, VP reactions of the $C_2H_4F_2$ complex, and the behavior of the system under matrix isolation conditions.

II. Potential-Energy Surface

The potential energy surface used in the present calculations has been described in detail elsewhere.[8] In this section, we briefly review some of the qualitative features of this surface that are particularly relevant to the present calculations. The reader is referred to ref 8 for a mathematical description of the surface and for a more detailed evaluation of its accuracy and topography.

In addition to reactions R1, R3, R4, and R5, various other channels are open on the surface. These include

$$C_2H_4 + F_2 \rightarrow CH_2{=}CHF + HF \tag{R6}$$

$$CH_2FCH_2F \rightarrow CH_2CH_2F + F \tag{R7}$$

$$CH_2FCH_2F \rightarrow CH_2{=}CH_2 + 2F \tag{R8}$$

$$CH_2FCH_2F \rightarrow CH_2{=}CHF + H + F \tag{R9}$$

$$CH_2FCH_2F \rightarrow CH_2FCHF + H \tag{R10}$$

$$CH_2FCH_2F \rightarrow CHF{=}CHF + 2H \tag{R11}$$

The reaction

$$CH_2{=}CH_2 + F_2 \rightarrow CH_2{=}CH + HF + F \tag{R12}$$

is also open on the surface. Its calculated endothermicity is 12.796 kcal/mol, so for higher energy collisions the channel is energetically accessible.

The calculated equilibrium geometries, reaction exothermicities, and fundamental vibration frequencies for the nonradical reactants and products are in fair-to-good agreement with measured values. The accuracy for the radical products is less.

III. Method and Results

The techniques employed in the quasi-classical trajectory calculations have been discussed in several review articles.[9-11] The methods used in the present calculations are fully described in ref 11.

The initial states of F_2 are selected quasi-classically from canonical distributions by the procedure described by Porter, Raff, and Miller for a rotating Morse oscillator.[12] Vibrational phase averaging is done by using the appropriate distribution function given in ref 12. The initial-state averaging for C_2H_4 is done as follows: The initial rotational state is obtained by assuming the C_2H_4 rotational levels are described by a rigid-rotor quantization with a moment-of-inertia equal to that for C_2H_4 rotation about an axis perpendicular to the molecular plane. Vibrational energy is selected quasi-classically by a harmonic quantization. The initial vibrational energy is partitioned among the designated normal modes as kinetic energy with C_2H_4 in its equilibrium conformation. A trajectory is then integrated for a time equal to 260.3 vibrational periods of the C–H symmetric stretch (ν_1) and the "stored structure" procedure[11] used to effect the vibrational phase averaging. In one calculation, the vibrational phases were averaged over 520.6 ν_1 periods.

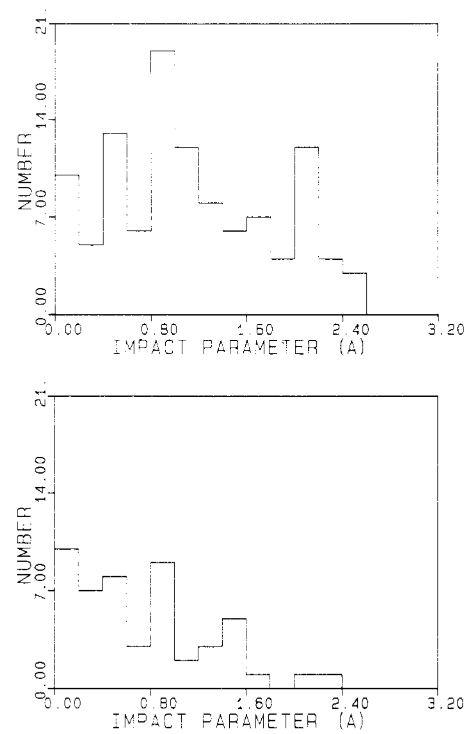

Figure 1. (A, top) Variation of the reaction probability with impact parameter for reaction R4. (B, bottom) Variation of the reaction probability with impact parameter for reaction R6.

TABLE I: Rotationally Averaged Reaction Cross Sections for Reactions R1, R4, R6, and R12 as a Function of Initial Relative Translational Energy[a]

		cross sections, Å^2			
E_{trans}, eV	N^b	R1	R4	R6	R12
1.046	662	0.0^c	1.64 ± 0.23	0.57 ± 0.13	0.0^c
1.356	282	0.0	2.81 ± 0.44	0.51 ± 0.35	0.0
1.634	192	0.0	4.49 ± 0.73	1.37 ± 0.41	0.0

[a] C_2H_4 and F_2 are initially in their ground vibrational states. Rotation is averaged at 300 K. Error limits represent 1 σ limit of statistical uncertainty. [b] Total number of trajectories computed. [c] No trajectories resulted in reactions R1 or R12. Zero entries therefore denote cross sections below the limit of detection for the present calculations.

Random initial orientation and rotation planes are introduced by using the usual rotation matrices.[11] In some cases, the initial relative speed was selected canonically; in other cases, the relative speed was fixed to allow reaction cross sections to be computed. The end tests were performed using a combination of distance and energy criteria. The 48 equations of motion were integrated with a fourth-order Runge–Kutta method with a fixed integration step of 1.019×10^{-16} s. Rotationally averaged reaction cross sections and rate coefficients at a given temperature were computed from batches of about 200–400 trajectories at each relative speed or temperature.

Importance sampling with an "expected distribution", $P_0 = 1/b$, was used in the selection of the impact parameter.[11,13] The maximum impact parameter was determined empirically. Parts A and B of Figure 1 show the variation of the reaction probability with impact parameter for reactions R4 and R6. Only one reaction to form CH_2CH_2F + F occurred with an impact parameter greater then 2.5 Å. The largest impact parameter for which $CH_2{=}CHF$ + HF formation was obtained was 1.7 Å. Consequently, we have used 2.5 Å as the maximum impact parameter in all calculations.

Final-state distributions, reaction cross sections, and rate coefficients are obtained from the trajectory results in the usual manner.[11] However, it is necessary to take into account that, because of the importance sampling used in the selection of the

---

[9] Porter, R. N.; Raff, L. M. In *Modern Theoretical Chemistry*; Miller, W. H., Ed.; Plenum: New York, 1976; p 1.

[10] Truhlar, D. G.; Muckerman, J. T. *Atom–Molecule Collision Theory: A Guide for the Experimentalist*; Bernstein, R. B., Ed.; Plenum: New York, 1979; p 505.

[11] Raff, L. M.; Thompson, D. L. In *Theory of Chemical Reaction Dynamics*; Baer, M., Ed.; CRC: Boca Raton, FL, 1985; Vol. III, p 1.

[12] Porter, R. N.; Raff, L. M.; Miller, W. H. *J. Chem. Phys.* **1972**, *63*, 2214.

[13] Faist, M. B.; Muckerman, J. T.; Schubert, F. E. *J. Chem. Phys.* **1978**, *69*, 4087.

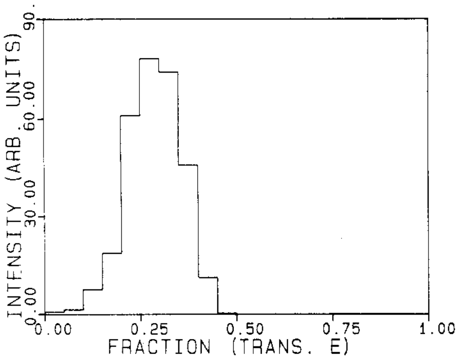

Figure 2. Final-state distribution of relative translational energy plotted as a function of the fraction of the total available energy appearing as relative translational motion for nonreactive $C_2H_4 + F_2$ collisions.

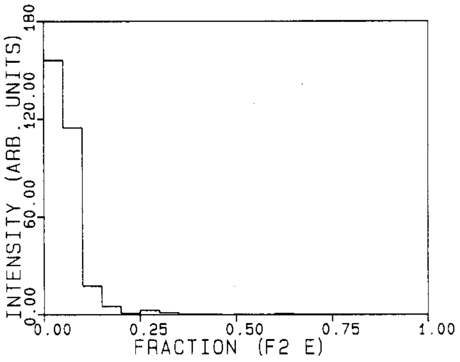

Figure 3. Final-state distribution of internal F_2 energy plotted as a function of the fraction of the total available energy appearing as internal F_2 energy for nonreactive $C_2H_4 + F_2$ collisions.

impact parameter, each trajectory is weighted by ξ_k, where ξ_k is the random number associated with the impact parameter in the kth trajectory:

$$b_k = \xi_k b_{\max} \tag{1}$$

Reaction Cross Sections and Final-State Distributions. Rotationally averaged reaction cross sections for reactions R1, R4, R6, and R12 have been computed at three different relative speeds with C_2H_4 and F_2 in their vibrational ground states. The rotational motion was averaged at 300 K. The results with associated statistical uncertainties are given in Table I. Almost all of the trajectories investigated are nonreactive. The reaction cross sections are all less than 5 Å^2 even when the translational energy is more than 1 eV in excess of the reaction threshold. The small steric factors associated with the addition of F_2 across the double bond are primarily responsible for this low reaction probability.

The major product of the bimolecular gas-phase reaction is $CH_2CH_2F + F$, in agreement with the experimental observations reported by Kapralova et al.[3] and with the general observed behavior of fluorine addition to olefins.[4,5] This is true for all reaction conditions which we have examined in the present studies. It is interesting to note that no 1,2-difluoroethane product with a lifetime greater than 2.55×10^{-12} s was obtained in any trajectory. As discussed in more detail below, this product was found as a short-lived intermediate, but not as a final product. In this regard, the gas-phase dynamics are markedly different from those observed under matrix isolation conditions.[1] Although several reaction channels leading to the formation of atomic hydrogen are energetically open, none of the trajectories gave this product.

Figures 2–4 show the final-state distributions of available energy between relative $F_2 + C_2H_4$ translation, internal F_2 motion, and internal C_2H_4 energy, respectively, for nonreactive trajectories with an initial relative translational energy of 1.0457 eV. Initially, about 56% of the available energy is present in the form of internal C_2H_4 motion and 41% as relative $F_2 + C_2H_4$ translation. These results show the collisions to be moderately inelastic with energy generally being transferred from translation into the internal C_2H_4 modes and, to some extent, into internal F_2 motion. The first moments of the distributions shown in Figures 2–4 are 0.29, 0.058, and 0.65, respectively.

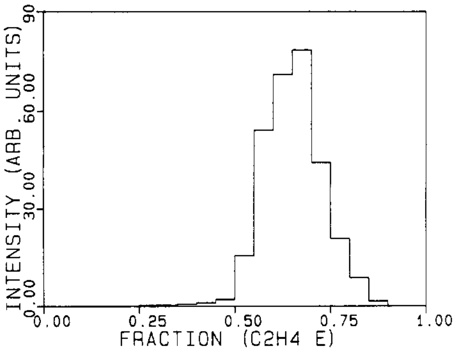

Figure 4. Final-state distribution of internal C_2H_4 energy plotted as a function of the fraction of the total available energy appearing as internal C_2H_4 energy for nonreactive $C_2H_4 + F_2$ collisions.

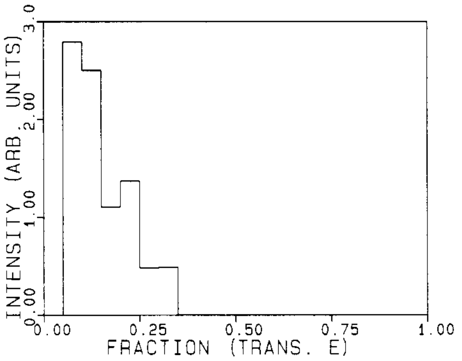

Figure 5. Same as Figure 2 for $HF + CH_2{=}CHF$ relative translational motion in $C_2H_4 + F_2$ collisions resulting in reaction R6.

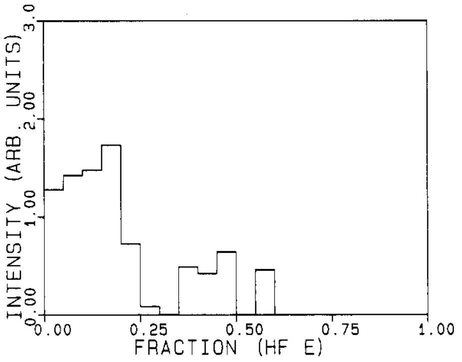

Figure 6. Final-state distribution of internal HF energy plotted as a function of the fraction of the total available energy appearing as internal HF energy for $C_2H_4 + F_2$ collisions resulting in reaction R6.

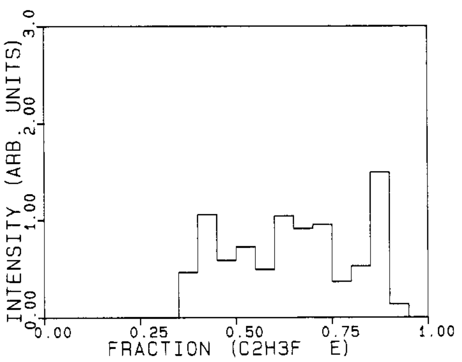

Figure 7. Final-state distribution of internal $CH_2{=}CHF$ energy plotted as a function of the fraction of the total available energy appearing as internal C_2H_3F energy for $C_2H_4 + F_2$ collisions resulting in reaction R6.

The potential energy surface used in the present calculations predicts an exothermicity for reaction R6 of 102.3 kcal/mol.[8] The

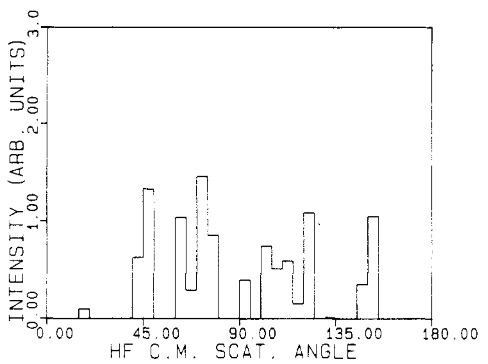

Figure 8. Center-of-mass differential cross section for HF products in reaction R6 with an initial relative translational energy of 1.0457 eV. C_2H_4 and F_2 are initially in their vibrational ground states. Scattering angles are given relative to the direction of the initial relative velocity vector.

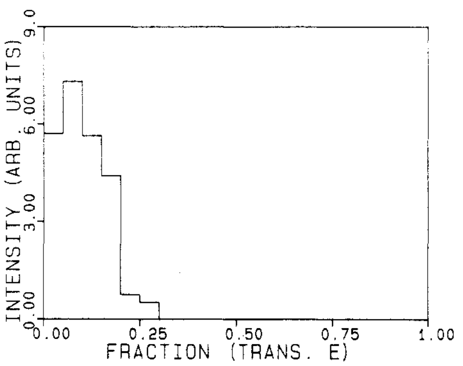

Figure 9. Final-state distribution of relative translational energy plotted as a function of the fraction of the total available energy appearing as relative translational motion for reaction R4.

total energy available to the $CH_2{=}CHF + HF$ products of reaction R6 is therefore about 160 kcal/mol, which includes 1.0457 eV of initial translational energy plus the internal energies of F_2 and C_2H_4. Figures 5–7 show the final-state distributions of this total energy for trajectories which react in channel R6. In contrast to the frequently observed result of very exothermic atom–molecule exchange reactions where the diatomic exchange product is often formed in highly excited vibrational states, Figure 5 shows that the HF product is usually formed in either the $v = 0$, 1, or 2 vibrational state, although vibrational states up to $v = 7$ or 8 are obtained. The average internal energy is 32 kcal/mol, which corresponds approximately to the $v = 2$ state. Very little of the available energy is partitioned into relative translational motion as shown by the final-state distribution given in Figure 6. On the average, $HF + CH_2{=}CHF$ translation accounts for 24 kcal/mol of the available energy, which is essentially equal to the amount initially in translational motion. Most of the reaction exothermicity is released as internal energy of the fluoroethylene product. Figure 7 shows that, on the average, internal $CH_2{=}CHF$ motion accounts for 65% of the total energy.

Figure 8 gives the center-of-mass differential cross section of HF products for reaction R6 for an initial relative translational energy of 1.0457 eV with C_2H_4 and F_2 in their vibrational ground states. The scattering angles are given relative to the direction of the initial relative velocity vector. The small number of reactive trajectories makes it difficult to draw more than qualitative conclusions. The distribution is rather isotropic between 45° and 145°, suggesting the formation of a complex.

On the present potential energy surface, reaction R4 is exothermic by 2.4 kcal/mol. The total available energy is therefore about 60.0 kcal. Figures 9 and 10 show the final-state distributions of this energy between relative translational and internal C_2H_4F motion, respectively. Translational $F{-}C_2H_4F$ motion accounts for an average of 10% of this energy. Consequently, the reaction process partitions most of the initial translational energy into internal C_2H_4F modes.

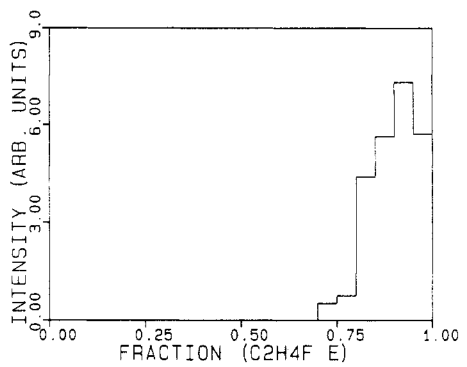

Figure 10. Final-state distribution of internal CH_2CH_2F energy plotted as a function of the fraction of the total available energy appearing as internal CH_2CH_2F energy for reaction R4.

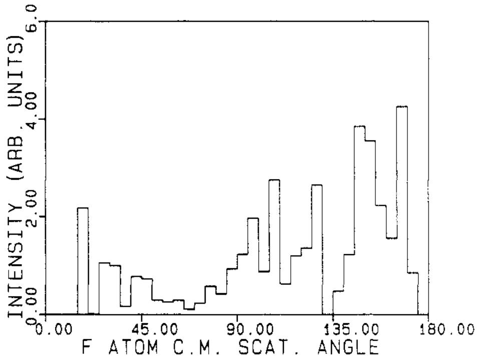

Figure 11. Center-of-mass differential cross section for F atom products in reaction R4 with an initial relative translational energy of 1.0457 eV. C_2H_4 and F_2 are initially in their vibrational ground states. Scattering angles are given relative to the direction of the initial relative velocity vector.

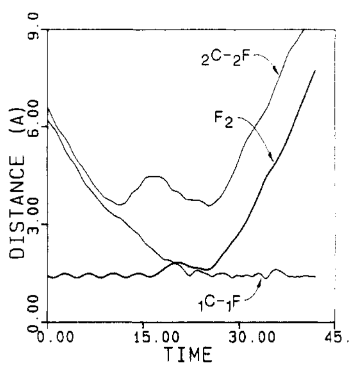

Figure 12. Typical direct R4 reaction. Distances are given in angstroms. One time unit corresponds to 1.019×10^{-14} s.

The center-of-mass differential cross section for fluorine atom scattering in reaction R4 is given in Figure 11. The distribution exhibits a large backscattered component corresponding to a rebound mechanism in which a fluorine atom is added across the C=C double bond while the second fluorine atom is scattered backwards along the direction of the initial relative velocity vector. There is also a smaller forward peak present that corresponds to F atom scattering in the direction of the incident relative velocity vector. Except for a few peaks between 90° and 135°, which may be statistical noise, the distribution is rather flat between 30° and 135°. These features suggest that three modes of reaction are present: (1) a stripping mechanism occurring at larger impact parameters in which one fluorine atom is abstracted and added across the C_2H_4 double bond while the second fluorine atom continues along its initial path, (2) a rebound mechanism at smaller impact parameters, and (3) a mechanism involving complex formation which results in more isotropic scattering.

Reaction Mechanisms. The mechanistic details of the reactive trajectories are very complex. The differential cross sections suggest that reaction R4 proceeds either through complex for-

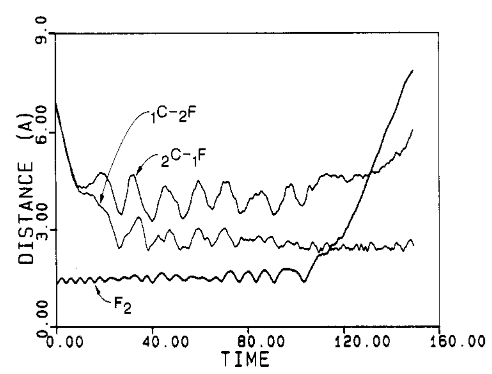

Figure 13. R4 reaction via $C_2H_4F_2$ complex formation. Distances are given in angstroms. One time unit corresponds to 1.019×10^{-14} s. The C–F distance is displaced upwards by 1.0 Å to provide visual clarity.

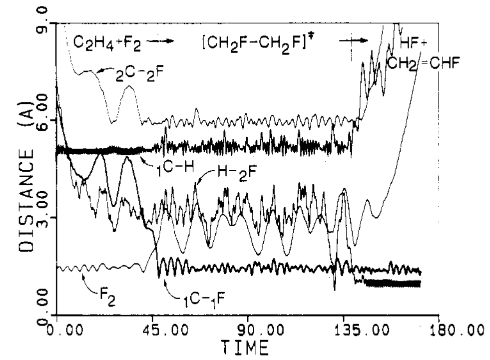

Figure 14. Trajectory resulting in reaction R6. Distances are given in angstroms. One time unit corresponds to 1.019×10^{-14} s. The $_1$C–H and $_2$C–$_2$F distances are displaced upwards by 3.5 and 4.5 Å, respectively, to provide additional visual clarity.

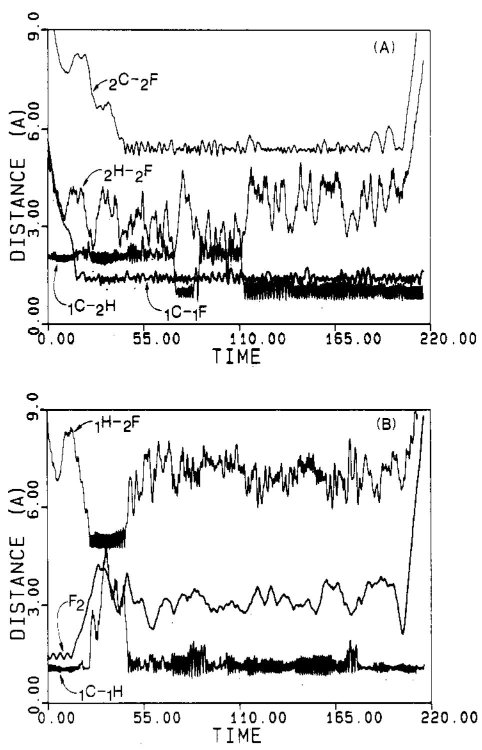

Figure 15. Trajectory resulting in reaction R6. Distances are given in angstroms. One time unit corresponds to 1.019×10^{-14} s. (A, top) $_1$C–$_2$H and the $_2$C–$_2$F distances have been displaced upwards by 0.5 and 3.5 Å, respectively, to provide additional visual clarity. (B, bottom) $_1$H–$_2$F distance has been displaced upward by 4.0 Å to provide additional visual clarity.

mation or by a direct stripping or rebound mechanism while reaction R6 involves complex formation. Examination of individual trajectories shows these conclusions to be correct. Figures 12 and 13 illustrate the two mechanisms which lead to reaction R4. A typical direct reaction is shown in Figure 12. The C–F distance is seen to decrease as F_2 approaches. As soon as F_2 is within the reaction radius, the F–F bond breaks, a fluorine atom is added across the double bond forming the C–F bond, and the second fluorine atom scatters immediately. The fact that the reaction is nearly thermochemically neutral is reflected in the nearly identical vibrational amplitudes seen for the F–F and C–F bonds. In contrast, Figure 13 illustrates formation of C_2H_4F via a complex. In this case, the interaction of F_2 with the C_2H_4 double bond results in the formation of a $C_2H_4F_2$ complex. (In the figure, the C–F bond distance has been displaced upwards by 1.0 Å to provide visual clarity.) Initially, this complex essentially has the two fluorine atoms bonded with the C–F bond only partially formed. This may be seen by noting the F_2 vibration frequency is nearly unaltered while the C–F frequency is initially very much less than that for a normal C–F bond. This complex lives for approximately 7.6×10^{-13} s. After 5.7×10^{-13} s, one fluorine atom forms a C–F bond, which begins to vibrate with the characteristic C–F frequency, while at the same time the F_2 bond weakens, causing F_2 dissociation. Since the lifetime of the complex is on the order of the average rotational period at 300 K for C_2H_4, this type of process will result in nearly isotropic scattering.

Figures 14 and 15 show the details of two typical trajectories which result in reaction R6. In this case, it is necessary to show the time variation of several interparticle distances to follow the mechanistic details of the reaction. We have therefore displaced some of the distances upwards, as noted in the figure captions, to produce more visual clarity in the plots. The mechanism illustrated in Figure 14 is typical. F_2 reaches the reaction zone 35 tu (time units; 1 tu = 1.019×10^{-14} s) after the start of the trajectory. At this point, the F_2 bond dissociates, the fluorine atoms add across the C=C double bond, and 1,2-difluoroethane forms. At this instant, the molecule contains approximately 160 kcal/mol of internal excitation. The increase in vibrational amplitudes produced by this energy is obvious in the figure. In this trajectory, 1,2-difluoroethane lives for about 85 tu (8.67×10^{-13} s) after which one of the C–H bonds on carbon atom no. 1 dissociates along with the simultaneous cleavage of the C–F bond on carbon atom no. 2, resulting in the four-center elimination of HF. The small vibrational amplitude of the HF bond is often characteristic of this type of trajectory as shown by the final-state HF energy distribution given in Figure 5.

Parts A and B of Figure 15 show an even more complex trajectory, which eventually leads to the formation of HF and fluoroethylene. The F_2 molecule is seen to dissociate approximately 20 tu after the start of the trajectory. Fluorine atom no. 1 forms a C–F bond with carbon no. 1 while the second fluorine atom attempts to abstract hydrogen no. 1 from carbon no. 1 to form hydrogen fluoride. This HF molecule actually forms and lives for about 20 tu. However, the internal HF energy is large and the process reverses. At 50 tu from the start of the trajectory, 1,2-difluoroethane forms with fluorine no. 2 bonded to carbon no. 2. This molecule retains its structure for about 20 tu after which a hydrogen migration from carbon no. 1 to fluorine no. 2 occurs. A partial H- -F bond forms momentarily, but the process is then seen to reverse, forming 1,2-difluoroethane 85 tu into the trajectory. At 110 tu, the same hydrogen migration again occurs. This time the process does not reverse. Hydrogen fluoride forms causing H–F bond rupture 200 tu into the trajectory, which completes the four-center dissociation of 1,2-difluoroethane. In this trajectory, the HF molecule is formed with 1.34 eV of internal excitation, which corresponds to the $v = 2$ vibrational state.

The lifetimes of 1,2-difluoroethane formed in the trajectories are less than 2.55×10^{-12} s. The above two examples are typical. Studies of the canonical and microcanonical dissociation rates for 1,2-difluoroethane, which are currently in progress, show that when the internal energy is statistically distributed the lifetimes are significantly longer than those observed in the present calculations. In addition, dissociation channels leading to products other than fluoroethylene and HF are observed. The implication of these results is that 1,2-difluoroethane formed by the reaction of C_2H_4

TABLE II: Thermal Rate Coefficients for Reactions R4 and R6[a]

temp, K	N[b]	rate coefficients, $cm^3/(mol \cdot s) \times 10^{-12}$ R4	R6
1500	179	1.47 ± 0.51	0.46 ± 0.25
2000	425	4.25 ± 1.76	1.24 ± 0.89
2500	192	9.27 ± 3.44	2.00 ± 1.37

[a] The error limits correspond to 1 σ limit of statistical uncertainty. [b] Number of trajectories computed.

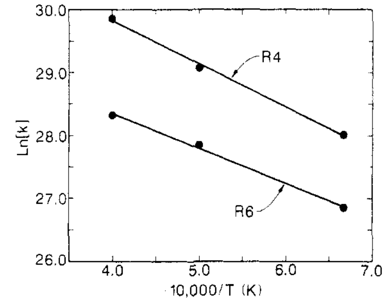

Figure 16. Arrhenius plots of the calculated thermal rate coefficients for reactions R4 and R6.

+ F_2 does not live for a sufficient period to achieve a statistical distribution of internal energy. These points will be discussed in greater detail in a subsequent paper dealing specifically with this subject.

Thermal Rate Coefficients. Kapralova et al.[3] have reported thermal rates for reaction R4 in the temperature range 300–437 K. The small reaction cross sections for this process make the computational requirements for the calculation of a thermal rate coefficient in this temperature range excessive. These calculations have therefore been carried out for temperatures between 1500 and 2500 K. The results for reactions R4 and R6 are given in Table II. Neither 1,2-difluoroethane nor $CH_2{=}CH$ is observed as a final product in any of the trajectories. Consequently, the rates for reactions R1 and R12 are too small to permit computation by the present methods.

Arrhenius plots of the data for reactions R4 and R6 are shown in Figure 16. The linear least-squares fits of this data yield activation energies of 13.6 and 11.04 kcal/mol, respectively, for reactions R4 and R6. The corresponding frequency factors are 1.38×10^{14} and 1.90×10^{13} $cm^3/(mol \cdot s)$, respectively. The gas-kinetic collision frequency for a maximum impact parameter of 2.5 Å is 9.24×10^{14} $cm^3/(mol \cdot s)$. Consequently, the trajectory calculations predict steric factors of 0.15 and 0.021 for reactions R4 and R6, respectively. The smaller steric factor, and corresponding smaller activation entropy, for reaction R6 is not unexpected since the mechanistic studies show that reaction R6 generally proceeds via complex formation whereas reaction R4 often involves a direct process.

The above results for reaction R4 are in disagreement with the data reported by Kapralova et al.[3] Their diffusion flame measurements suggest an activation energy for R4 of 4.6 kcal/mol and a frequency factor of 4.82×10^{13} $cm^3/(mol \cdot s)$. These differences could be the result of inaccuracies in the $C_2H_4F_2$ potential energy surface, errors in the experimental measurements or interpretation of the data, or effects produced by the different temperature ranges explored in the experiments and the calculations.

Effects of Vibrational Excitation. Rotationally averged reaction cross sections for reactions R4 and R6 have been computed at a relative translational energy of 1.046 eV for various initial C_2H_4 vibrational states whose characteristics are summarized in Table III. In each case, rotation was averaged at 300 K for a relative translational energy of 1.046 eV. The results are given in Table IV. None of the trajectories resulted in either 1,2-difluoroethane or $CH_2{=}CH$ being formed.

No mode specificity for the formation of HF via reaction R6 is observed. The calculated cross sections for this reaction are, within the statistical error limits of the study, the same for excitation of ν_1, $\nu_2 + \nu_{12}$, ν_3, ν_4, ν_5, ν_6, ν_7, or ν_9 with 0.35–0.39 eV of energy above zero-point energy. The cross section obtained when mode ν_6 is excited is somewhat lower than that for excitation of the other modes. However, it lies within most of the combined statistical error limits.

TABLE III: C_2H_4 Vibrational Modes

mode	description	freq, cm^{-1}
ν_1	symmetric C–H stretch	3019
ν_2	symmetric CH_2 band	1623
ν_3	carbon–carbon symmetric stretch	1342
ν_4	torsional motion	825
ν_5	asymmetric C–H stretch	3272
ν_6	planar CH_2 rock	1050
ν_7	nonplanar CH_2 rock	949
ν_8	nonplanar asymmetric CH_2 rock	943
ν_9	asymmetric C–H stretch	3106
ν_{10}	planar CH_2 rock	995
ν_{11}	asymmetric C–H stretch	2990
ν_{12}	asymmetric CH_2 bend	1444

TABLE IV: Reaction Cross Sections for Vibrationally Excited States of C_2H_4[a]

excited vib state[b]	total[c] E_{vib}, eV	N[d]	cross sections, Å^2 R4	R6
	C–H Stretching			
$\nu_1 = 1.5$	0.374	119	3.95 ± 0.82	0.95 ± 0.48
$\nu_9 = 1.5$	0.385	156	2.57 ± 0.61	1.07 ± 0.37
$\nu_5 = 1.5$	0.406	387	2.65 ± 0.39	1.13 ± 0.26
	C–C Stretching			
$\nu_3 = 2.75$	0.374	188	1.71 ± 0.46	1.01 ± 0.34
	CH_2 Bend and Rocking			
$\nu_2 = \nu_{12} = 1.5$	0.380	234	1.48 ± 0.3	0.78 ± 0.27
$\nu_6 = 3.38$	0.375	169	2.10 ± 0.54	0.29 ± 0.16
	Out-of-Plane			
$\nu_7 = 3.5$	0.353	182	1.89 ± 0.47	1.04 ± 0.36
$\nu_4 = 4.16$	0.374	152	2.26 ± 0.55	0.78 ± 0.27

[a] Rotational states are averaged at 300 K. The relative translational energy is 1.046 eV. The error limits correspond to 1 σ limit of statistical uncertainty. [b] Nominal vibrational quantum number. All other $\nu_i = 0$. [c] Internal C_2H_4 energy in excess of zero-point energy. [d] Total number of trajectories computed.

In contrast, it appears that there may be some mode-specific rate enhancement for reaction R4. In this case, initial partitioning of the C_2H_4 internal energy into the C–H stretching modes is more effective in promoting the formation of the fluoroethyl radical than partitioning an equal amount of energy into either the C=C stretch or most of the CH_2 bending or rocking modes. The out-of-plane C_2H_4 torsional mode, ν_4, and the planar CH_2 rock, ν_6, appear to be intermediate between the C–H stretching modes and the other bending and rocking modes in enhancing the cross section for reaction R4.

Although the differences in the cross sections for F + CH_2CH_2F formation computed for excitation of the various modes lie outside the combined statistical error limits corresponding to 1 σ limit, the differences are small enough that they could be the result of statistical error outside of 1 σ limit. In addition, there is the possibility of systematic bias in the initial C_2H_4 vibrational phase averaging. The initial phases were randomly sampled over 260 ν_1 vibrational periods. This amount of phase space, while large, may still be insufficient to accurately represent the C_2H_4 vibrational motion. Consequently, while the present results suggest the presence of mode specificity in reaction R4, it is small and may possibly be the result of statistical and/or sampling errors.

These results are very different from those observed by Frei, Fredin, and Pimentel[1] under matrix isolation conditions. The total vibrational rate enhancement observed in the present studies amounts to a factor of 3 or less, whereas in the matrix experiments[1] the quantum efficiency of the process was found to increase by as much as 5 orders of magnitude as the photon wavenumber increased from 953 to 4209 cm^{-1}. Such a difference is not unexpected, however, since in the gas-phase calculations the relative translational energy is 1.046 eV in contrast to its near zero value in the matrix experiments.[1] Consequently, the percentage increase in total available energy upon vibrational excitation is much greater in the matrix than in the gas-phase reaction.

Mode specificity was observed by Frei et al.[1] in their matrix studies of the $C_2H_4 + F_2$ reaction. However, it too is different than that found in the present calculations. In the matrix, excitation of the $v_2 + v_{12}$ combination band at 3076 cm^{-1} was found to yield a quantum efficiency greater than that for excitation of v_9 at 3105 cm^{-1}. In the gas phase, this behavior is reversed with v_9 being more effective than the combination excitation. Since even the products of the gas-phase reaction are different than those observed under matrix isolation conditions, it is not surprising that the detailed dynamics of the two processes are likewise completely different.

IV. Summary

A quasi-classical trajectory study of the bimolecular reaction dynamics for the reaction of F_2 with ethylene has been carried out on a previously described potential energy surface[8] on which all important reaction channels are open. The surface yields equilibrium geometries, reaction exothermicities, and fundamental vibrational frequencies in fair-to-good accord with measured values.

The major reaction products of the gas-phase collision of F_2 with C_2H_4 are found to be CH_2CH_2F and fluorine atoms. The secondary products are HF and $CH_2{=}CHF$. 1,2-Difluoroethane is never found as a final product although it is observed as an intermediate in the reaction leading to the formation of $CH_2{=}CHF$.

The calculated reaction cross sections are all less than 5 Å^2 even when the translational energy is more than 1 eV in excess of the reaction threshold. The small cross sections are primarily the result of the demanding steric requirements for these reactions. The corresponding thermal rate coefficients for the two principal reactions are too small to permit trajectory calculation at 300 K. Over the range $1500\ \text{K} \leqslant T \leqslant 2500\ \text{K}$, they are found to be $1.38 \times 10^{14} \exp[-13\,600/RT]$ and $1.90 \times 10^{13} \exp[-11\,040/RT]$ cm^3/(mol·s) for the formation of CH_2CH_2F and $CH_2{=}CHF$, respectively.

Virtually all of the reaction exothermicity is partitioned into the internal modes of CH_2CH_2F or $CH_2{=}CHF$. Very little energy appears in the form of relative translational motion of the products. HF is usually formed in the $v = 0$, 1, or 2 vibrational state. The calculated center-of-mass differential cross section for F atom scattering shows a strong backward component along with an isotropic component. Examination of individual trajectories shows that the first of these arises from a direct reaction mechanism while the second is the result of complex formation. Formation of $CH_2{=}CHF$ is shown to occur via a complex mechanism involving the formation of 1,2-difluoroethane as an intermediate.

No evidence is found for mode-specific rate enhancement of the reaction leading to the formation of $CH_2{=}CHF$. However, there is some evidence for its presence in the reaction forming the fluoroethyl radical. In this case, excitation of the C–H stretching modes seems to be more efficient in promoting the reaction than a similar excitation of the either the C=C stretch or the CH_2 bending or rocking modes. The magnitude of the effect, however, is small and could be the result of statistical or sampling error.

The dynamics of the gas-phase reaction of $C_2H_4 + F_2$ are found to be very different from those observed by Frei et al.[1] in their study of this reaction under matrix isolation conditions.

Acknowledgment. All calculations in this paper were carried out on a VAX 11/780 and a microVAX II purchased, in part, with funds provided by grants from the Department of Defense University Instrumentation Program, AFOSR-85-0115, and the Air Force Office of Scientific Research, AFOSR-86-0043.

Registry No. C_2H_4, 74-85-1; F_2, 7782-41-4; $CH_2{=}CHF$, 75-02-5; CH_2CH_2F, 28761-00-4; FCH_2CH_2F, 624-72-6; H, 1333-74-0.

Study of the Complexation Kinetics of Cs^+ Ion with Dibenzo-30-crown-10 in Some Nonaqueous Solvents by ^{133}Cs NMR

Mojtaba Shamsipur[1] and Alexander I. Popov*

Department of Chemistry, Michigan State University, East Lansing, Michigan 48824

(Received: May 12, 1987)

The exchange kinetics of the complexation of the cesium ion with dibenzo-30-crown-10 were studied in nitromethane, acetonitrile, propylene carbonate, and methanol solutions by cesium-133 NMR line-shape analysis. In the last three solvents, when the temperature is below −10 °C, the predominant mechanism for the exchange of the Cs^+ ion between the solvated and complexed sites is the bimolecular process. In nitromethane solutions, at all temperatures studied, and in propylene carbonate and methanol solutions at −10 °C, the exchange process proceeds by the dissociation pathway. The activation parameters E_a, $\Delta H^{\ddagger}$, $\Delta S^{\ddagger}$, and $\Delta G^{\ddagger}$ for the exchange have been determined. In systems where the exchange mechanism is bimolecular, the free energy barrier for the exchange process appears to be independent of the solvent.

Introduction

Among the macrocyclic crown ethers synthesized by Pedersen,[2] ligands with large rings such as dibenzo-30-crown-10 are particularly interesting. These ligands are quite flexible, and the rings are large enough to twist around a metal ion of proper size and form three-dimensional, "wrap-around" complexes. Such structures have been reported for crystalline dibenzo-30-crown-10 complexes with potassium[3] and rubidium[4] ions. Experimental evidence for the existence of a "wrap-around" structure for the complexes between this ligand and K^+ and Cs^+ ions in various nonaqueous solvents has also been reported.[5,6]

---

[1] On leave from the Department of Chemistry, Razi University, Bakhtaran, Iran.

(2) Pedersen, C. J. *J. Am. Chem. Soc.* **1967**, *89*, 7017.

(3) Bush, M. A.; Truter, M. R. *J. Chem. Soc., Perkin Trans. 2* **1972**, *2*, 345.

(4) Hasek, J.; Huml, K.; Hlavata, D. *Acta Crystallogr., Sect. B* **1979**, *B35*, 330.

(5) Live, D.; Chan, S. I. *J. Am. Chem. Soc.* **1976**, *98*, 3769.

0022-3654/88/2092-0147$01.50/0